DOI 10.1007/s11182-015-0416-x

Russian Physics Journal, Vol. 57, No. 11, March, 2015 (Russian Original No. 11, November, 2014)

SPATIOTEMPORAL DYNAMICS OF WIND VELOCITY FROM MINI-SODAR MEASUREMENTS

N. P. Krasnenko,[1,2] M. V. Tarasenkov,[3] and L. G. Shamanaeva[3] UDC 551.501.755 + 551.501.796

Mini-sodar measurements of wind velocity profiles in the 20–200 m layer have demonstrated the high efficiency of the use of mini-sodars in monitoring the fine structure of the atmospheric boundary layer (ABL) and in detecting jets and wind shear. An analysis of measurements of vertical profiles of the wind velocity and its vertical and horizontal components has shown that analytical approximations of the vertical profile of the horizontal wind velocity are possible for both neutral and unstable stratifications of the atmosphere. They are well described by a logarithmic law. The approximation constants are found and the errors associated with their use are estimated. The established physical trends and the obtained constants for the horizontal and vertical components of the wind velocity allow a description of their hourly and daily dynamics and can be recommended for use in ABL models intended for prognostic calculations (forecasting). The vector representation makes it possible to visualize the spatiotemporal dynamics of the wind field in the atmospheric boundary layer, in particular to estimate the shape and size of jets and wind shear in them.

Keywords: wind velocity, acoustic sounding, atmospheric boundary layer.

Studies of trends in the behavior of the wind velocity in the ABL have both fundamental [1–5] and applied significance [6]. Wind is the most variable meteorological parameter of the atmosphere. Knowledge of the vertical profiles of the wind velocity as well as the dynamics of their variation is important. Vertical motions also play a large role in atmospheric processes. Real-time data on wind velocity profiles are needed to refine short-range weather forecasts, to predict the state of the air basin (to estimate pollutant concentrations and pollutant transport) in various regions, to provide a weather service to airports (most importantly, to determine wind shear with the aim of ensuring the safety of takeoffs and landings), etc. Whereas measurements of wind profiles in the atmospheric surface layer have reached a high stage of development, thanks in large measure to short meteorological masts equipped with sensors at various heights, and models of wind behavior in the surface layer do exist, the situation is more complicated in the boundary layer. The Monin–Obukhov similarity theory was developed for the surface layer, according to which the wind velocity profiles and likewise other meteorological quantities are defined in terms of universal functions that depend on the type of stratification of the atmosphere and on the roughness of the underlying surface. The wind profile in the ABL also depends on the geostrophic wind velocity (i.e., on conditions in the free atmosphere). Construction of a general theory of the ABL, similar to the above-mentioned theory for the surface layer, would be quite laborious due to multifactor dependences.

To measure the vertical profile of the wind velocity and construct, on the basis of such measurements, some kind of theory of the ABL and calculational models based on it [1], use was made primarily of tall meteorological masts [2, 3] equipped with meteorological sensors at selected suitable altitudes. For example, in Obninsk automated sensors

[1]Institute of Monitoring of Climatic and Ecological Systems of the Siberian Branch of the Russian Academy of Sciences, Tomsk, Russia; [2]Tomsk State University of Control Systems and Radio Electronics, Tomsk, Russia; [3]V. E. Zuev Institute of Atmospheric Optics of the Siberian Branch of the Russian Academy of Sciences, Tomsk, Russia, e-mail: krasnenko@imces.ru; tmv@iao.ru; sima@iao.ru. Translated from Izvestiya Vysshikh Uchebnykh Zavedenii, Fizika, No. 11, pp. 77–83, November, 2014. Original article submitted July 22, 2014.

were positioned at altitudes of 10, 121, and 301 m [2, 3] while on the mast at Boulder (Colorado), such sensors were positioned at altitudes of 10, 100, and 300 m [5]. These do not provide high spatial resolution and, consequently, do not reveal the fine structure of the wind field in the ABL. Also, because they are fixed in place they can only be used to make measurements under conditions of a fixed underlying surface.

For real-time measurements of wind field characteristics in the ABL, remote sensing systems employing radio, optical, and acoustic waves are more suitable. Acoustic sounding is preferable for this purpose. Possessing higher capabilities in regard to spatial resolution, it allows one to study the fine structure of the ABL [7, 8]. The strong interaction of sound waves with the atmosphere (for example, the refractive index of sound waves is roughly 10^6 times greater than for optical waves) and the possibility of obtaining information in real time around the clock with substantially greater spatial and temporal resolution make acoustic radars a unique instrument for studying the atmospheric boundary layer. And the application of high-frequency monostatic three-component Doppler radars (mini-sodars) to measure the wind velocity vector makes it possible to obtain long time series of continuous observations with high spatial (down to several meters) and temporal resolutions (statistically reliable wind profiles are achievable with averaging, as a rule, over time intervals ranging from 10 to 30 min) and to analyze their spatiotemporal dynamics. This makes mini-sodars a suitable instrument for making real-time measurements that constitute a basis for subsequent development of models of the behavior of the wind velocity in the ABL. The problem of developing models of the behavior of the vertical profile of the wind velocity and its variations is of current interest.

As inputs to our analysis we used the results of measurements of an AV4000 monostatic Doppler mini-sodar with a 50-element phased antenna array [9]. The working frequency of the mini-sodar was 4900 Hz, the duration of the radiation pulse was 60 ms, and the pulse repetition period was 4 s. The radiation was sequentially transmitted and received in three directions – the vertical direction and two directions inclined at an angle $\alpha = 18°$ to the vertical in two mutually orthogonal planes. Three components of the wind velocity vector were measured. Their altitude profiles $V_x(z_k)$, $V_y(z_k)$, and $V_z(z_k)$ were calculated from the Doppler shifts of the frequencies $f_{1D}(z_k)$, $f_{2D}(z_k)$, and $f_{3D}(z_k)$, respectively, in three channels (of transmission and reception) from the formulas [8]

$$V_z(z_k) = \frac{c}{2f_0} f_{1D}(z_k), V_1(z_k) = \frac{c}{2f_0} f_{2D}(z_k), \; V_2(z_k) = \frac{c}{2f_0} f_{3D}(z_k),$$
$$V_x(z_k) = \frac{1}{\sin\alpha}\left[V_1(z_k) - V_z(z_k)\cos\alpha\right], V_y(z_k) = \frac{1}{\sin\alpha}\left[V_2(z_k) - V_z(z_k)\cos\alpha\right]. \quad (1)$$

Measurements were taken in the altitude range 20–200 m. The weather was dry, warm, and sunny, and the underlying surface was even and devoid of tall vegetation. The components of the wind velocity in 40 strobes z_k of vertical extent $\Delta z = 5$ m each were determined. Mini-sodar data from 6 days of measurements during the autumnal (late-summer) period from 12 to 17 September were processed and analyzed. Series of 150 profiles each were processed, which ensured averaging of the data over 10-minute measurement periods.

As an example, the hourly half-day dynamics of the *x* and *y* components of the wind velocity and the average horizontal wind velocity, measured on 13 September from 11:00 to 11:10 (*a*), 13:00 to 13:10 (*b*), 15:00 to 15:10 (*c*), 18:00 to 18:10 (*d*), 20:00 to 20:10 (*e*), and from 22:00 to 22:10 (*f*) local time are shown in Fig. 1. On this day, in distinction to the others, quite smooth profiles of the horizontal wind velocity were recorded although on the whole nonstationarity of processes taking place in the ABL is observed, where this nonstationarity is due first of all to the diurnal course of incident solar radiation. It can be seen from Fig. 1 that the average wind velocity $V_{av}(z)$ grows with altitude *z*, and that starting at 18:00 its growth slows down. The variability of the wind velocity over the course of a day is connected with the variation of the character of the stratification of the ABL. In the lower layer the maximum wind velocities were observed around noon and in the afternoon; in the upper layers minimum wind velocities were observed at the indicated times.

The obtained altitude profiles of the average horizontal wind velocity are well approximated by the logarithmic dependence

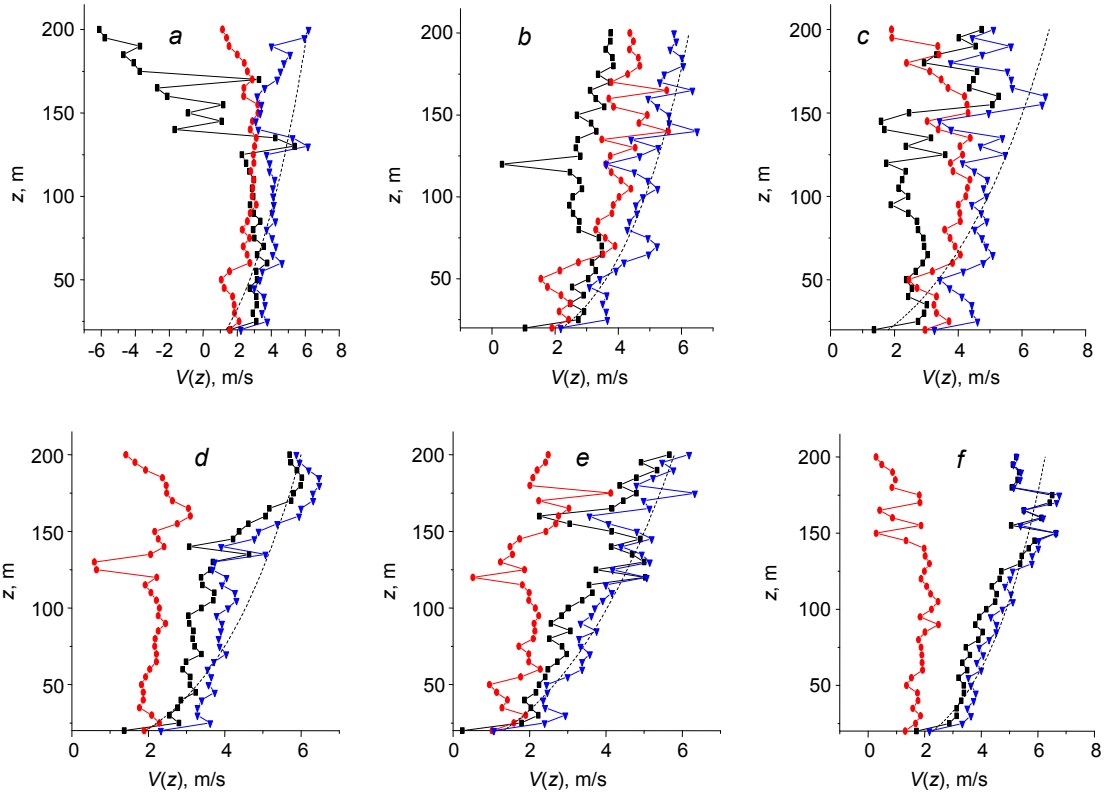

Fig. 1. Half-day dynamics of V_x (rectangles) and V_y (rhombuses) of the components of the wind velocity and average horizontal wind velocity V_{av} (triangles) from mini-sodar measurements over the course of one day, 13 September; the dotted curve plots the approximation V_{av} found using formula (2).

$$V_{\text{av}}(z) = \left(\frac{\ln(z)}{A}\right)^{1/N}. \tag{2}$$

The corresponding approximation is shown by the dotted line in Fig. 1. The values of the approximation constants are listed in Table 1. The available models [1] developed for neutral stratification of the ABL (which is valid, first of all, for strong winds, in the afternoon, in cloudy weather), as a rule, use a logarithmic law of variation of the wind velocity with altitude. A more general form is a simple power law, where the parameter of this law should be assigned with allowance for stratification of the ABL, the wind velocity at 10 m, roughness of the underlying surface, and thickness of the atmospheric layer under consideration.

Approximation errors were estimated as follows. The standard deviation is given by the formula

$$\text{STD} = \sqrt{\frac{1}{N}\sum_{i=1}^{N}(V_i - V_{\text{av}i})^2}. \tag{3}$$

The maximum absolute error is given by the formula

$$M = \max_{i=1,N} |V_i - V_{\text{av}i}|, \tag{4}$$

TABLE 1. Approximation Constants in Formula (2)

Measurement time	A	N
11:00–11:10 (*a*)	2.68	$3.76 \cdot 10^{-1}$
12:00–12:10	1.81	$6.32 \cdot 10^{-1}$
13:00–13:10 (*b*)	1.91	$5.56 \cdot 10^{-1}$
14:00–14:10	2.31	$4.44 \cdot 10^{-1}$
15:00–15:10 (*c*)	2.33	$4.27 \cdot 10^{-1}$
16:00–16:10	2.23	$4.86 \cdot 10^{-1}$
17:00–17:10	3.01	$1.93 \cdot 10^{-1}$
18:00–18:10 (*d*)	2.68	$3.88 \cdot 10^{-1}$
19:00–19:10	1.56	$6.94 \cdot 10^{-1}$
20:00–20:10 (*e*)	2.15	$5.04 \cdot 10^{-1}$
21:00–21:10	3.34	$2.11 \cdot 10^{-1}$
22:00–22:10 (*f*)	1.87	$5.67 \cdot 10^{-1}$

TABLE 2. Errors in Approximation of the Horizontal Wind Velocity Using Formulas (3) and (4)

Measurement time	STD, m/s	M, m/s
11:00–11:10 (*a*)	7.35	2.30
12:00–12:10	2.88	$9.82 \cdot 10^{-1}$
13:00–13:10 (*b*)	3.55	1.58
14:00–14:10	3.45	1.20
15:00–15:10 (*c*)	7.68	2.78
16:00–16:10	2.75	1.11
17:00–17:10	2.41·10	1.01·10
18:00–18:10 (*d*)	3.10	1.61
19:00–19:10	4.31	1.59
20:00–20:10 (*e*)	3.83	1.39
21:00–21:10	1.46·10	7.53
22:00–22:10 (*f*)	3.11	1.06

where V_i is the measured value of the velocity, and $V_{\text{av}i}$ is the approximate value. Calculated values of the approximation errors are given in Table 2. It can be seen that formula (2) adequately describes the half-day dynamics of the average horizontal wind velocity; the maximum approximation error corresponds to the profile measured from 21:00 to 21:10.

Figure 2 shows the corresponding half-day dynamics of the vertical component of the wind velocity. The approximation was based on a third-order polynomial:

$$V_z(z) = Bz^3 + Cz^2 + Dz + E\,. \tag{5}$$

The approximation constants are given in Table 3. It can be seen from Fig. 2 that V_z was negative during the measurement times, which is evidence of motion of air masses away from the underlying surface. Moreover, in the profile of the vertical component of the wind velocity a minimum is distinctly traced out, whose altitude varies from 70 to 150 m over the duration of the measurements.

The approximation errors for the vertical component of the wind velocity are listed in Table 4. It should be remarked that the maximum approximation error corresponds to the profile measured from 20:00 to 20:10. It is clear

TABLE 3. Approximation Constants for the Vertical Component of the Wind Velocity in Formula (5)

Measurement time	B	C	D	E
11:00–11:10 (*a*)	$9.31\cdot10^{-8}$	$-1.85\cdot10^{-5}$	$2.60\cdot10^{-4}$	$-6.22\cdot10^{-2}$
12:00–12:10	$-7.53\cdot10^{-8}$	$2.48\cdot10^{-5}$	$-1.92\cdot10^{-3}$	$-1.13\cdot10^{-1}$
13:00–13:10 (*b*)	$2.13\cdot10^{-7}$	$-6.58\cdot10^{-5}$	$5.64\cdot10^{-3}$	$-2.06\cdot10^{-1}$
14:00–14:10	$1.23\cdot10^{-7}$	$-3.82\cdot10^{-5}$	$3.24\cdot10^{-3}$	$-1.67\cdot10^{-1}$
15:00–15:10 (*c*)	$-2.40\cdot10^{-7}$	$9.19\cdot10^{-5}$	$-9.77\cdot10^{-3}$	$7.79\cdot10^{-2}$
16:00–16:10	$9.01\cdot10^{-8}$	$-2.84\cdot10^{-5}$	$2.84\cdot10^{-3}$	$-1.65\cdot10^{-1}$
17:00–17:10	$5.93\cdot10^{-8}$	$-1.04\cdot10^{-5}$	$3.81\cdot10^{-4}$	$-1.83\cdot10^{-1}$
18:00–18:10 (*d*)	$-2.22\cdot10^{-7}$	$8.71\cdot10^{-5}$	$-8.89\cdot10^{-3}$	$-2.88\cdot10^{-3}$
19:00–19:10	$-1.36\cdot10^{-7}$	$5.19\cdot10^{-5}$	$-5.23\cdot10^{-3}$	$-1.38\cdot10^{-2}$
20:00–20:10 (*e*)	$-7.78\cdot10^{-8}$	$3.27\cdot10^{-5}$	$-4.33\cdot10^{-3}$	$1.10\cdot10^{-1}$
21:00–21:10	$1.12\cdot10^{-7}$	$-3.08\cdot10^{-5}$	$2.13\cdot10^{-3}$	$-1.29\cdot10^{-1}$
22:00–22:10 (*f*)	$-1.83\cdot10^{-7}$	$6.13\cdot10^{-5}$	$-5.20\cdot10^{-3}$	$-1.51\cdot10^{-2}$

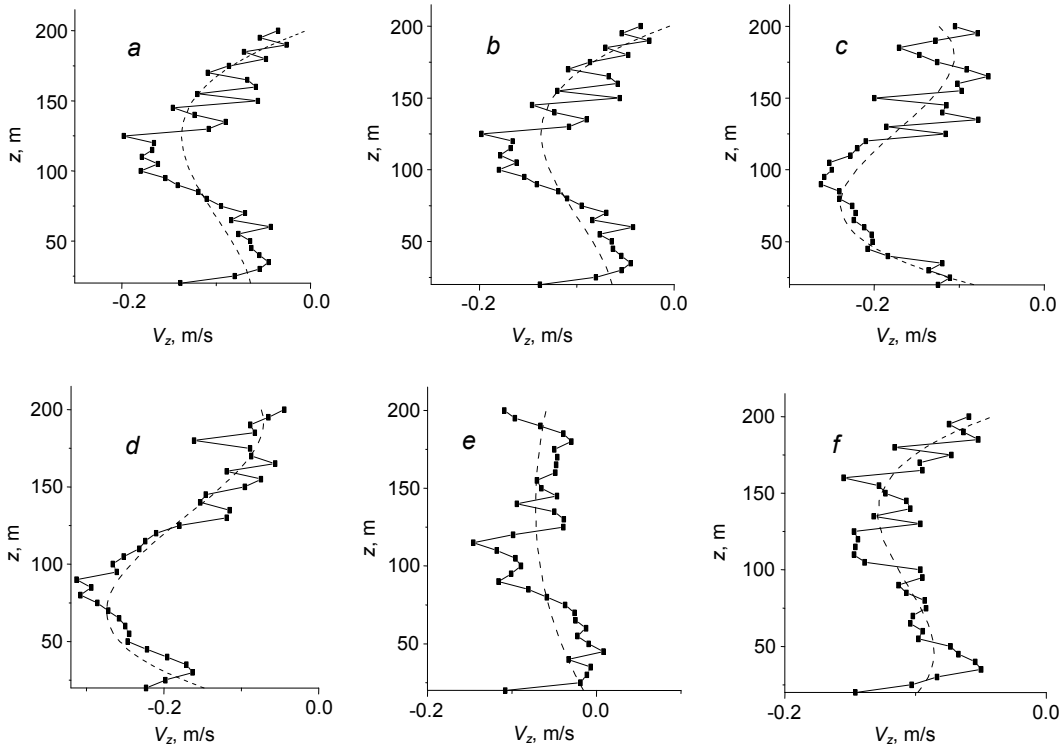

Fig. 2. Half-day dynamics of the vertical component of the wind velocity from mini-sodar measurements during one day, 13 September; the dotted curve plots the approximation V_{av} found using formula (5).

from Table 4 that formula (5) adequately describes the half-day spatiotemporal dynamics of the vertical component of the wind velocity.

Figure 3 shows a vector representation of the half-day spatiotemporal dynamics of the horizontal wind velocity based on mini-sodar measurements taken on 14 and 16 September. It can be seen from Fig. 3*a* that at 11 hours local time the vertical distribution of the wind velocity was quite uniform, directed northeast, and preserved that character over the entire range of sounding altitudes. As can be seen from this graphic, V_h initially grew with altitude, and its

TABLE 4. Errors in Approximation of the Vertical Component of the Wind Velocity Using Formulas (3) and (4)

Measurement time	STD, m/s	M, m/s
11:00–11:10 (*a*)	$2.00 \cdot 10^{-1}$	$7.44 \cdot 10^{-2}$
12:00–12:10	$1.36 \cdot 10^{-1}$	$4.51 \cdot 10^{-2}$
13:00–13:10 (*b*)	$1.76 \cdot 10^{-1}$	$5.72 \cdot 10^{-2}$
14:00–14:10	$1.52 \cdot 10^{-1}$	$5.47 \cdot 10^{-2}$
15:00–15:10 (*c*)	$1.99 \cdot 10^{-1}$	$8.06 \cdot 10^{-2}$
16:00–16:10	$1.14 \cdot 10^{-1}$	$6.24 \cdot 10^{-2}$
17:00–17:10	$1.93 \cdot 10^{-1}$	$8.97 \cdot 10^{-2}$
18:00–18:10 (*d*)	$1.94 \cdot 10^{-1}$	$8.46 \cdot 10^{-2}$
19:00–19:10	$1.62 \cdot 10^{-1}$	$7.12 \cdot 10^{-2}$
20:00–20:10 (*e*)	$2.22 \cdot 10^{-1}$	$1.44 \cdot 10^{-1}$
21:00–21:10	$1.26 \cdot 10^{-1}$	$4.77 \cdot 10^{-2}$
22:00–22:10 (*f*)	$1.67 \cdot 10^{-1}$	$8.59 \cdot 10^{-2}$

maximum value was reached at an altitude of 75 m. From that point onward it decreased smoothly with altitude z. This is characteristic of stable stratification (the presence of a temperature inversion). At the upper boundary of the inversion the wind profile has a jet-like character. The inversion rises and then decays. The stratification changes from stable to unstable, but in the afternoon, to neutral. At 12 hours local time, the quite uniform distribution of V_h was maintained up to the altitude $z = 175$ m, and the wind velocity also grew with altitude. At 13 hours local time, the northeastward direction of V_h changed over to southwestward and stayed that way until about 17 hours. At 18 hours, the direction of the horizontal component of the wind changed over to northwestward, but the altitude of the upper boundary of the jet in the surface layer decreased with time and was equal to 75 m at 23 hours. Note that at nightfall a stable stratification of the atmosphere is formed once again and strong jets are observed at altitudes of 100 and 160 m. The overall picture of trends in the behavior of V_h points to the presence of a Bénard–Rayleigh convection cell, observed above the warmer underlying surface during the time interval over which the measurements were taken. As can be seen from the measurements, the construction of one simple model for the behavior of the wind velocity for different states of the ABL is extraordinarily difficult.

From the measurement data on 16 September the wind was stronger, especially in the lower 100-meter layer. Here an increase in the altitude of the maximum of V_h is tracked from 45 m at 10 hours local time to 100 m at 14 hours. This also is caused by a rise of the nocturnal surface temperature inversion. In the wind-velocity profile the presence of such a dangerous phenomenon for aviation as wind shear is distinctly observed [6]. At 18 hours the southwestward direction of the jet shifted to northwestward, and the altitude of the jet at first increased from 100 m at 20 hours to 125 m at 21 hours, and then decreased to 75 m at 22 hours. At 23 hours the wind direction shifted to southeastward, and the wind became weaker. The irregular behavior of the wind velocity in the lower 25-meter layer can be explained by the influence of roughness of the underlying surface and its irregular heating.

Thus, measurements of wind velocity profiles in the 20–200 m layer with mini-sodar have demonstrated its high efficiency in monitoring the fine structure of the ABL, revealing jets, and detecting wind shear. An analysis of the measurements of the altitude profiles of the wind velocity vector and its vertical and horizontal components has shown that analytical approximations of the vertical profile of the horizontal component of the wind velocity are possible for both neutral and unstable stratifications of the atmosphere. They are described quite well by a logarithmic law, as was noted earlier in the processing of wind velocity measurements made using tall meteorological masts. Approximation constants were found and the errors associated with their use have been estimated. For stable stratification of the atmosphere and, in particular, in the presence of elevated temperature inversions it is problematic to make such an approximation without a knowledge of additional characteristics of the ABL; in this case, it is necessary to perform real measurements. The established physical trends and the obtained approximation constants for the horizontal and vertical components of the wind velocity enable a description of their hourly and daily dynamics and can be recommended for use in models of the ABL and prognostic calculations (forecasting). The vector representation makes

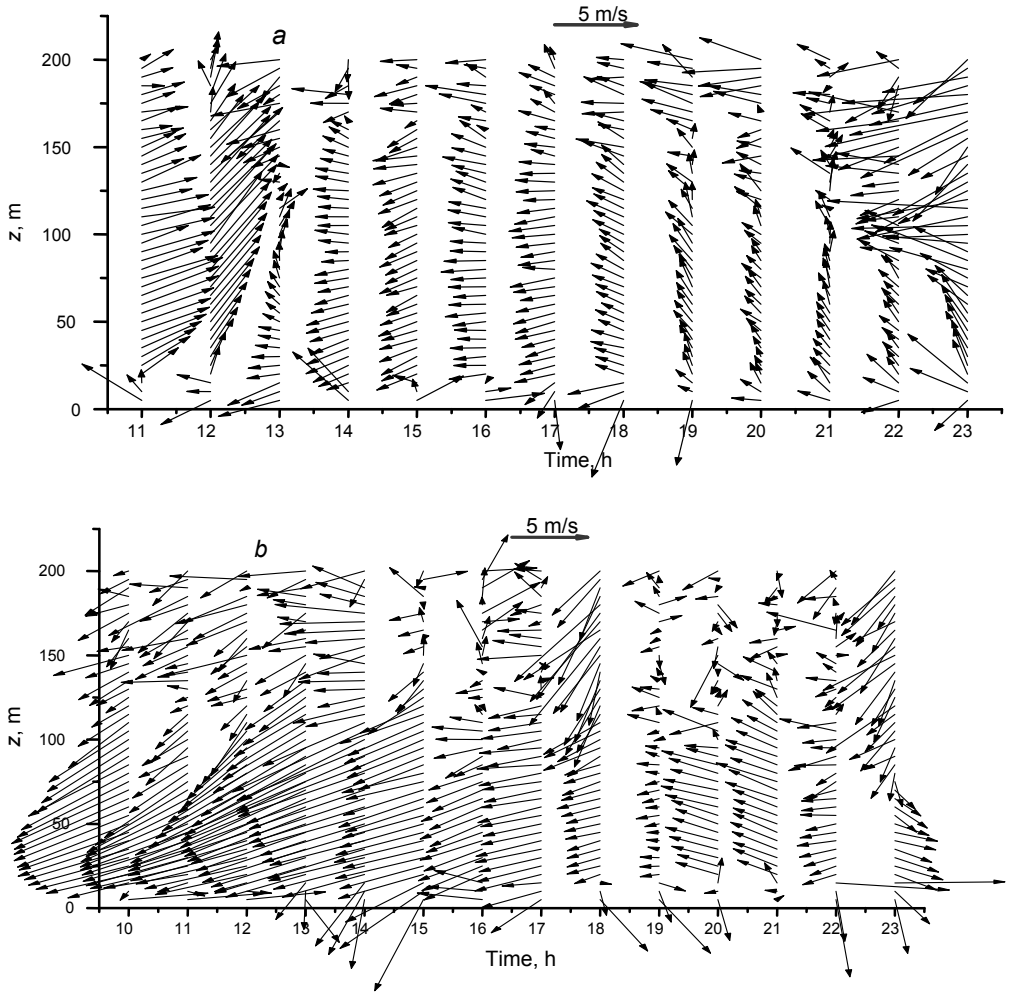

Fig. 3. Hourly half-day spatiotemporal dynamics of the horizontal wind velocity from mini-sodar measurements on 14 and 16 September. Orientation: upward is north, and to the left is west.

it possible to visualize the spatiotemporal dynamics of the wind field in the atmospheric boundary layer, in particular to estimate the shape and size of the jets and wind shear in them.

REFERENCES

1. Atmosphere. A Handbook [in Russian], Gidrometeoizdat, Leningrad (1991).
2. N. L. Byzova, ed., Standard Characteristics of the Lower 300-Meter Layer of the Atmosphere from Measurements on a Meteorological Mast [in Russian], Gidrometeoizdat, Moscow (1982).
3. N. L. Byzova, V. I. Ivanov, and E. K. Garger, Turbulence in the Atmospheric Boundary Layer [in Russian], Gidrometeoizdat, Leningrad (1989).
4. M. M. Borisenko, Vertical Profiles of Wind and Temperature in the Lower Layers of the Atmosphere, Trudy Glavn. Geofiz. Observ., No. 320 (1974).
5. M. A. Lokoshenko, Meteor. Gidrol., No. 4, 19–31 (2014).

6. P. D. Astapenko, A. M. Baranov, I. M. Shvarev, *et al*., Aviation Meteorology: Textbook [in Russian], Transport, Moscow (1979).
7. S. Bradley, Atmospheric Acoustic Remote Sensing: Principles and Applications, CRC Press, Boca Raton, FL (2007).
8. N. P. Krasnenko, Acoustic Sounding of the Atmospheric Boundary Layer [in Russian], Vodolei, Tomsk (2001).
9. http://minisodar.org.